

Showcasing research from Kyoko Nozaki's laboratory, The University of Tokyo, Japan.

Selective synthesis of unsymmetric dibenzo[a,e]pentalenes by a rhodium-catalysed stitching reaction

Dibenzo[a,e]pentalenes have attracted attention as stable  $\pi$ -conjugated molecules bearing narrow energy gaps, which are expected to be utilised in applications for optical and electronic devices. For the construction of a dibenzo[a,e]pentalene framework, we developed a rhodium-catalysed stitching reaction between 2-(silylethynyl)arylboronates and 2-(silylethynyl)aryl bromides. The introduction of appropriately sized silyl groups on the starting substrates led to a high crossover selectivity without using an excess amount of either substrate. The present stitching reaction could produce a variety of unsymmetric dibenzo[a,e]pentalene derivatives, including those with electronically different substituents on the fused benzene rings as well as heteroarene fused compounds.

As featured in:



See Shingo Ito, Ryo Shintani, Kyoko Nozaki et al., *Chem. Sci.*, 2017, 8, 101.



[rsc.li/chemical-science](http://rsc.li/chemical-science)

Registered charity number: 207890

CrossMark  
click for updatesCite this: *Chem. Sci.*, 2017, 8, 101

# Selective synthesis of unsymmetric dibenzo[*a,e*]pentalenes by a rhodium-catalysed stitching reaction†

Keisuke Takahashi, Shingo Ito,\* Ryo Shintani\* and Kyoko Nozaki\*

A rhodium-catalysed stitching reaction between 2-(silylethynyl)arylboronates and 2-(silylethynyl)aryl bromides has been developed for the synthesis of unsymmetric dibenzo[*a,e*]pentalenes. The introduction of appropriately sized silyl groups on the starting substrates led to a high crossover selectivity without using an excess amount of either substrate. The present stitching reaction could produce a variety of unsymmetric dibenzo[*a,e*]pentalene derivatives, including those with electronically different substituents on the fused benzene rings as well as heteroarene fused compounds. Desilylative halogenation was also demonstrated to synthesise the corresponding halogenated dibenzo[*a,e*]pentalenes, which can be used as building blocks for further chemical transformations.

Received 12th October 2016  
Accepted 2nd November 2016

DOI: 10.1039/c6sc04560j

www.rsc.org/chemicalscience

## Introduction

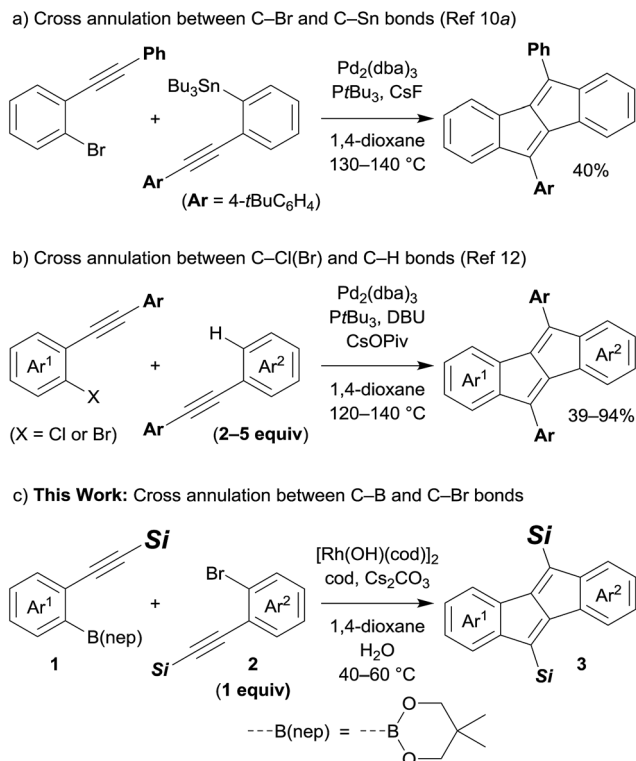
Pentalene has attracted much attention because of its anti-aromatic character, which is derived from its planar structure with  $8\pi$ -electrons.<sup>1</sup> However, due to its instability,<sup>2</sup> the construction of a pentalene framework often requires fusion of arene rings. Thus, dibenzo[*a,e*]pentalenes have been prepared and isolated as stable  $\pi$ -conjugated molecules bearing narrow energy gaps,<sup>3</sup> which are expected to be utilised in optical and electronic device applications.<sup>4</sup> For the construction of a dibenzo[*a,e*]pentalene framework, a variety of synthetic methods have been developed: intramolecular cyclisation of 5,6,11,12-tetradehydrodibenzo[*a,e*]cyclooctene derivatives,<sup>5</sup> reductive cyclisation of 1,4-diiodo-2,3-diaryl-1,3-butadienes<sup>6</sup> or di(2-arylphenyl)acetylenes,<sup>7</sup> and  $B(C_6F_5)_3$ -induced cyclisation of 1,2-bis(phenylethynyl)benzenes.<sup>8</sup> Transition metal complexes are also often used to synthesise dibenzo[*a,e*]pentalenes as exemplified by the nickel-mediated<sup>4a,d,9</sup> or palladium-catalysed<sup>4b,10</sup> reductive dimerisation of 2-alkynylaryl halides, palladium-catalysed oxidative dimerisation of arylacetylenes,<sup>11</sup> and palladium-catalysed cross annulations of 2-alkynylaryl halides.<sup>4c,10a,12</sup> Despite these significant advances, the synthesis of dibenzo[*a,e*]pentalene derivatives that are unsymmetrically fused by two different (hetero)arenes or ones that are unsymmetrically substituted have been less studied.<sup>4c,5e,f,10,12</sup> This

could be mainly due to difficulties in selective cross annulation between two different substrates. For example, Tilley and co-workers found that a palladium-catalysed reaction of 2-alkynylphenyl bromide and (2-alkynylphenyl)tributylstannane afforded the corresponding cross annulation product in moderate yields accompanied by the formation of homo-dimerisation products (Scheme 1a).<sup>10a</sup> As another example, Jin and co-workers reported palladium-catalysed cross annulations of 2-alkynylaryl chlorides and diarylacetylenes, which offer a general synthetic method to prepare various unsymmetric dibenzo[*a,e*]pentalene derivatives including heteroarene-fused pentalenes (Scheme 1b).<sup>12</sup> However, the use of an excess amount of diarylacetylenes is required in this catalyst system. To achieve a highly selective cross annulation to synthesise unsymmetric pentalene derivatives without using an excess amount of either substrate, the development of a new catalytic system would therefore be desired.

We recently developed a rhodium-catalysed stitching reaction, as a novel strategy for the intermolecular synthesis of polycyclic  $\pi$ -conjugated ladder-type compounds *via* successive insertion of alkynes.<sup>13,14</sup> This method allowed for the synthesis of quinoidal fused oligosiloles for the first time through the reaction of an oligo(silylene-ethynylene) containing an arylmetal moiety and a haloarene moiety at each end with another oligo(silylene-ethynylene) of an appropriate length. On the basis of this strategy, we envisaged that the construction of a dibenzo[*a,e*]pentalene structure could be achieved through a stitching reaction between alkyne **1** bearing an arylboron moiety and alkyne **2** bearing a bromoarene moiety in the presence of a rhodium catalyst (Scheme 1c). Herein we describe the successful synthesis of various unsymmetric dibenzo[*a,e*]pentalenes using this strategy. High crossover- and regioselectivities could be achieved through

Department of Chemistry and Biotechnology, Graduate School of Engineering, The University of Tokyo, 7-3-1 Hongo, Bunkyo-ku, Tokyo 113-8656, Japan. E-mail: ito\_shingo@chembio.t.u-tokyo.ac.jp; shintani@chembio.t.u-tokyo.ac.jp; nozaki@chembio.t.u-tokyo.ac.jp; Fax: +81-3-5841-7263; Tel: +81-3-5841-7261

† Electronic supplementary information (ESI) available: General, experimental, spectral, and theoretical information. CCDC 1511836–1511838. For ESI and crystallographic data in CIF or other electronic format see DOI: 10.1039/c6sc04560j



Scheme 1 Transition-metal-catalysed cross annulations to form unsymmetric dibenzo[*a,e*]pentalene derivatives.

proper differentiation of the size of silyl groups on each reaction component.

## Results and discussion

### Synthesis of dibenzo[*a,e*]pentalenes through the rhodium-catalysed stitching reaction

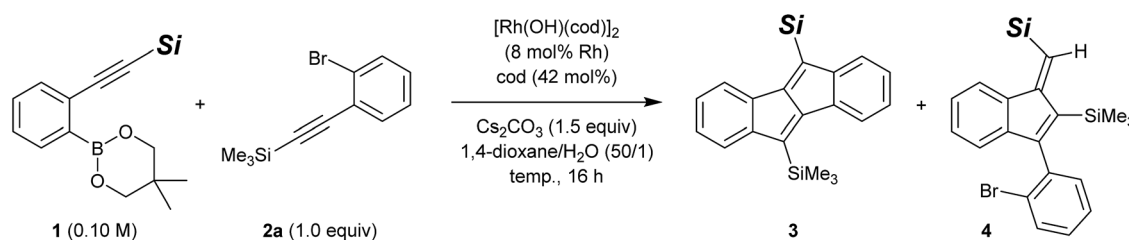
Considering the ease of post-functionalisation of the synthesised dibenzo[*a,e*]pentalenes, we chose 2-(silylethynyl)arylboronates (**1**) and 2-(silylethynyl)aryl bromides (**2**) as the substrate combination for the rhodium-catalysed stitching reaction. We initially employed equimolar amounts of 2-[(trimethylsilyl)ethynyl]phenylboronate (**1a**)<sup>15</sup> and [(2-bromophenyl)ethynyl]trimethylsilane (**2a**) and conducted the reaction in the presence of di- $\mu$ -hydroxidobis[(1,5-cyclooctadiene)rhodium] (8 mol% Rh), 1,5-cyclooctadiene (42 mol%), and cesium carbonate (1.5 equiv.) in 1,4-dioxane/water (50/1) at 60 °C (Table 1, entry 1).<sup>13</sup> Under these conditions, 83% of **1a** and 53% of **2a** were consumed after 16 h, and the desired dibenzo[*a,e*]pentalene **3aa** was obtained in 43% yield along with 2% yield of side-product **4aa** (*vide infra*). We subsequently found that the yield of **3** could be significantly improved through the use of boronate **1b** bearing a bulkier *tert*-butyldimethylsilyl group (**3ba**: 87% yield, **3ba/4ba** = 90/10; entry 2), but no further improvement was observed using boronate **1c** with an even bulkier triisopropylsilyl group (**3ca**: 48% yield; entry 3). For the reaction of **1b** and **2a**, raising the reaction temperature to 80 °C resulted in slightly lower yield and selectivity of **3ba** (79% yield,

**3ba/4ba** = 89/11; entry 4). By lowering the reaction temperature to 40 °C, in contrast, the selectivity of **3ba/4ba** was improved to 92/8 and the yield of **3ba** reached 90% (78% isolated yield; entry 5). An essentially identical result was obtained when the reaction was scaled up to a 0.50 mmol scale (entry 6). It is worth noting that the present rhodium-catalysed stitching reaction for the synthesis of dibenzo[*a,e*]pentalene efficiently proceeds at a low temperature of 40 °C, which is in stark contrast to reported palladium-catalysed reactions that usually require high reaction temperatures of 120–140 °C.<sup>10,12</sup>

A proposed catalytic cycle for the present reaction of **1b** with **2a** to form **3ba** is illustrated in Scheme 2, left. Initially, the transmetalation of arylboronate **1b** with rhodium(i) complex **A** forms arylrhodium intermediate **B**. Alkenylrhodium species **C** is then generated through the intermolecular insertion of **2a** into the carbon–rhodium bond of **B**<sup>16</sup> in an orientation that forms a carbon–carbon bond at the silylated carbon of **2a**. Successive intramolecular insertion of the alkyne into the carbon–rhodium bond of **C** gives intermediate **D**.<sup>17</sup> Finally, the intramolecular oxidative addition of bromoarene gives **E** and subsequent carbon–carbon bond-forming reductive elimination produces dibenzo[*a,e*]pentalene **3ba** along with the regeneration of rhodium(i) complex **A**.<sup>18</sup> Side-product **4ba** is presumably formed through the insertion of **2a** into the carbon–rhodium bond of **B** in the opposite regioselectivity, forming a carbon–carbon bond at the arylated carbon of **2a** to give intermediate **C'**. This then undergoes intramolecular alkyne insertion to give intermediate **D'**, protonolysis of which leads to **4ba** with the regeneration of rhodium(i) complex **A**. The formation of undesired **4ba** could be suppressed to some extent by conducting the reaction at a lower temperature (Table 1, entries 2, 4, and 5).

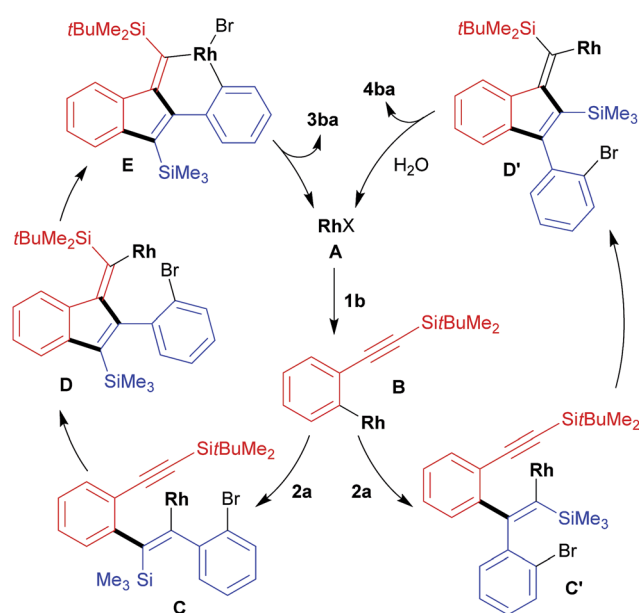
The high crossover selectivity of the present stitching reaction led us to examine the scope using various 2-[(*tert*-butyldimethylsilyl)ethynyl]arylboronates (**1**) and 2-[(trimethylsilyl)ethynyl]aryl bromides (**2**) (Scheme 3). In addition to the synthesis of **3ba**, the present method was also effective for the synthesis of  $\pi$ -extended pentalenes such as benzo[*a*]naphtho[2,3-*e*]pentalene **3bb** (74% yield) and dinaphtho[2,3-*a*:2',3'-*e*]pentalene **3db** (63% yield). Both electron-rich aryl bromide **2c** and electron-deficient aryl bromide **2d** were also applied to afford the corresponding dibenzopentalenes **3bc** and **3bd** in 41% yield and 69% yield, respectively, although both reactions had to be carried out at 60 °C for 32 h to reach full conversion. In this catalysis, bromides at other positions in compounds **2** are tolerated because the reaction is initiated by the transmetalation of an arylboronate rather than the oxidative addition of an aryl bromide (see Scheme 2). For example, trimethyl[(2,4,5-tribromophenyl)ethynyl]silane **2e** could be used in the reaction with **1b** to give dibromodibenzopentalene **3be** in 74% yield. With the aim of obtaining donor–acceptor type pentalenes, the use of electron-rich arylboronate **1e** bearing a dimethylamino group was also examined. The reaction of **1e** with **2a** successfully gave **3ea**, albeit in a moderate yield of 34% with full conversion of both substrates. Similarly, by combining arylboronate **1e** and aryl bromide **2d**, donor–acceptor type pentalene **3ed**, bearing a dimethylamino group and a nitro group on



Table 1 Optimisation of the reaction of 2-(silylethynyl)phenylboronate (**1**) with [(2-bromophenyl)ethynyl]trimethylsilane (**2a**)<sup>a</sup>


Entry	1	Temp. (°C)	Product	3 <sup>b</sup> (%)	4 <sup>b</sup> (%)	Recovery of 1 <sup>b</sup> (%)	Recovery of 2a <sup>b</sup> (%)
1	1a (Si = SiMe <sub>3</sub> )	60	3aa	43	2	17	47
2	1b (Si = Si <i>t</i> BuMe <sub>2</sub> )	60	3ba	87	10	0	0
3	1c (Si = Si <i>i</i> Pr <sub>3</sub> )	60	3ca	48	6	18	31
4	1b	80	3ba	79	10	0	0
5	1b	40	3ba	90 (78)	8	0	0
6 <sup>c</sup>	1b	40	3ba	87 (77)	8	0	0

<sup>a</sup> Reaction conditions: a mixture of **1** (0.10 mmol), **2a** (0.10 mmol), [Rh(OH)(cod)]<sub>2</sub> (8 μmol Rh), cod (42 μmol), and Cs<sub>2</sub>CO<sub>3</sub> (0.15 mmol) in 1,4-dioxane/H<sub>2</sub>O (50/1; 1.0 mL) was stirred for 16 h at the indicated temperature. <sup>b</sup> Yields were determined using <sup>1</sup>H NMR analysis against an internal standard (CH<sub>2</sub>Br<sub>2</sub>). The isolated yields are shown in parentheses. <sup>c</sup> The reaction was conducted on a 0.50 mmol scale.



Scheme 2 Proposed catalytic cycles for the reaction of **1b** with **2a** to form dibenzo[*a,e*]pentalene **3ba** and side-product **4ba** (Rh = Rh(cod) and X = OH or Br).

each aromatic ring, was obtained in 36% yield. In addition, the present method could be extended to the synthesis of the pyridine-fused pentalene, benzo[*a*]pyrido[2,3-*e*]pentalene **3bf**, in a high yield (81% yield).

The present catalysis could also be applied to the synthesis of benzothienopentalenes, although the yields are not particularly high (Scheme 4). Thus, benzothienopentalenes **3bg** and **3bh** were isolated in 20% yield and 23% yield, respectively, by employing corresponding thienyl bromides **2g** and **2h** in the reaction with arylboronate **1b** at 40 °C for 16 h. Somewhat

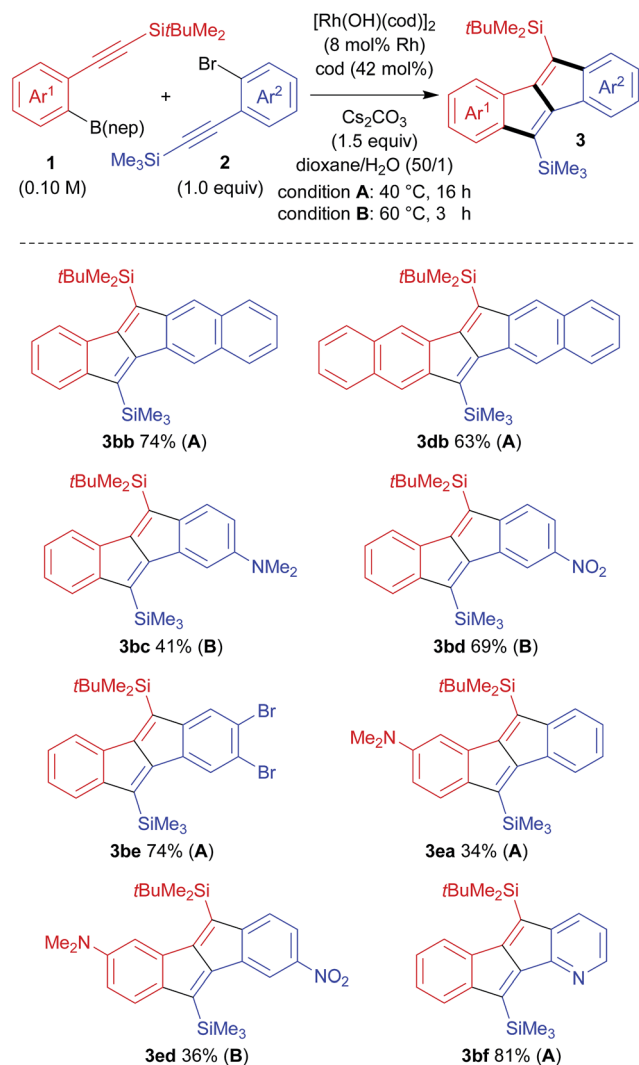
higher yields were achieved by conducting these reactions at 60 °C for 32 h, giving **3bg** in 50% <sup>1</sup>H NMR yield and **3bh** in 43% <sup>1</sup>H NMR yield along with the generation of inseparable side products including **4**. The synthesis of benzothienopentalenes could also be achieved using thienylboronates **1f** and **1g** with aryl bromide **2a**, giving **3fa** in 10% isolated yield and **3ga** in 41% <sup>1</sup>H NMR yield with inseparable side-products. Pyrido[2,3-*a*]thieno[3',2'-*e*]pentalene **3ff** and pyrido[2,3-*a*]thieno[2',3'-*e*]pentalene **3gf** were prepared in 48% yield and 20% yield, respectively, using pyridyl bromide **2f** as the reaction partner. This represents the first synthesis of pentalenes that are fused by two different heteroarenes, although the yields are still low to moderate.

### Selective desilylative halogenation

For the purpose of utilizing the obtained pentalenes as building blocks for further extended  $\pi$ -conjugated systems, the desilylative halogenation of compounds **3** was examined (Scheme 5). Thus, the treatment of benzonaphthopentalene **3bb** with bromine in diethyl ether at room temperature smoothly converted both of the silyl groups into bromides without brominating other positions, to give 5,12-dibromobenzo[*a*]naphtho[2,3-*e*]pentalene **5** in 71% yield. On the other hand, the reaction of **3bb** with iodine in tetrahydrofuran at 40 °C selectively converted only the trimethylsilyl group to an iodide, keeping the *tert*-butyldimethylsilyl group intact to give compound **6** in 77% yield. These halogenated pentalene derivatives could be of further use with the rich chemistry of organo halides, such as in cross-coupling reactions<sup>5b</sup> and nucleophilic substitution reactions.<sup>19</sup> This demonstrates that the present rhodium catalysis for the synthesis of unsymmetric dibenzo[*a,e*]pentalenes and the subsequent desilylative halogenation would be an efficient method for the preparation of pentalene-based functional molecules.



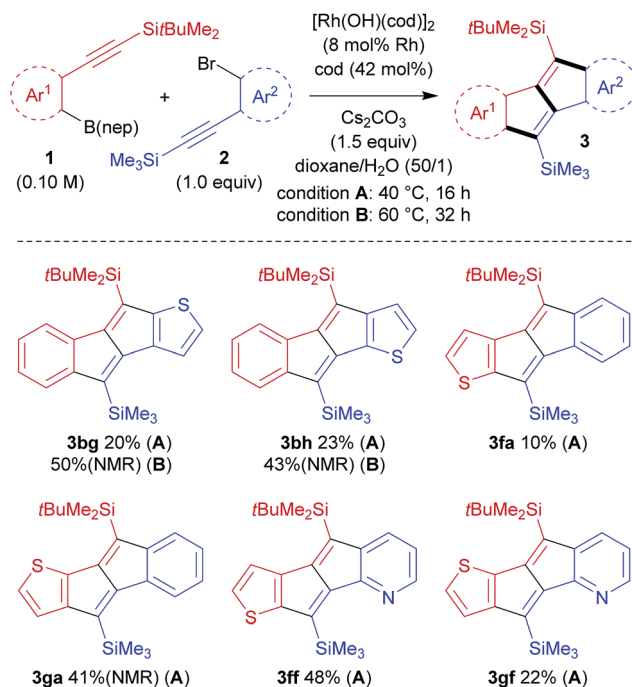




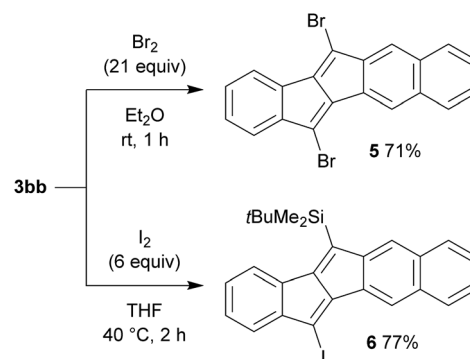
Scheme 3 Scope of the rhodium-catalysed stitching reaction for the synthesis of dibenzo[a,e]pentalene derivatives.

### Optical and electronic properties

With various dibenzopentalene derivatives (**3**) in hand, we evaluated their optical and electronic properties by UV-vis absorption spectroscopy and cyclic voltammetry (Table 2). UV-vis absorption spectra of the obtained pentalenes were obtained in dichloromethane (Fig. 1). Dibenzopentalene **3ba** exhibited an absorption maximum ( $\lambda_{\text{max}}$ ) at 444 nm ( $\epsilon_{\text{max}} = 1.0 \times 10^4 \text{ L mol}^{-1} \text{ cm}^{-1}$ ), and  $\lambda_{\text{max}}$  was shifted bathochromically and  $\epsilon_{\text{max}}$  increased as the number of fused rings increased in the order of **3bb** ( $\lambda_{\text{max}} = 478 \text{ nm}$  and  $\epsilon_{\text{max}} = 1.7 \times 10^4 \text{ L mol}^{-1} \text{ cm}^{-1}$ ) and **3db** ( $\lambda_{\text{max}} = 500 \text{ nm}$  and  $\epsilon_{\text{max}} = 1.9 \times 10^4 \text{ L mol}^{-1} \text{ cm}^{-1}$ ), owing to the extension of the  $\pi$ -conjugation (Fig. 1a). Time-dependent density functional theory (TD-DFT) calculations at the B3LYP/6-31G(d) level of theory suggested that the absorption band of **3ba** in the 350–550 nm region can be attributed to the HOMO–1  $\Rightarrow$  LUMO and HOMO  $\Rightarrow$  LUMO+1 transitions (Fig. S1 and Table S1†). In the case of **3ba**, the oscillator strength ( $f$ ) of the HOMO–LUMO transition was calculated to be zero ( $f = 0.0000$ ),



Scheme 4 Rhodium-catalysed stitching reaction to synthesise thienopentalenes.



Scheme 5 Desilylative halogenation of benzonaphthopentalene **3bb**.

which is consistent with the fact that the corresponding absorption was not observed.<sup>9a</sup>

The effect of functional groups, such as dimethylamino and nitro groups, was also investigated (Fig. 1b). The shape of the absorption spectrum of dibenzo[a,e]pentalene **3bd** bearing a nitro group resembled that of **3ba** with a small bathochromic shift of 11 nm ( $\lambda_{\text{max}} = 455 \text{ nm}$  and  $\epsilon_{\text{max}} = 1.5 \times 10^4 \text{ L mol}^{-1} \text{ cm}^{-1}$ ). This phenomenon could be explained by charge transfer absorption, similar to the relationship between benzene and nitrobenzene.<sup>20</sup> As was the case for **3ba**, the oscillator strength corresponding to the HOMO  $\Rightarrow$  LUMO transition of **3bd** was calculated to be nearly zero ( $f = 0.0012$ ), and the corresponding absorption was not observed. In contrast, the introduction of a dimethylamino group dramatically changed the shape of the absorption spectrum and generated a new broad absorption band in the longer wavelength region (**3ea**:  $\lambda_{\text{max}} = 613 \text{ nm}$  and



Table 2 Summary of the UV-vis absorption spectroscopy, cyclic voltammetry, and DFT calculations of pentalenes 3

Compound	$\lambda_{\max}$ [nm] ( $\epsilon_{\max}^a [\times 10^4 \text{ L mol}^{-1} \text{ cm}^{-1}]$ )	$E_{\text{ox}}^{\text{onsetb}}$ [eV]	$E_{\text{red}}^{\text{onsetb}}$ [eV]	$E_{\text{HOMO,CV}}^c$ [eV] ( $E_{\text{HOMO,cal}}^d$ [eV])	$E_{\text{LUMO,CV}}^c$ [eV] ( $E_{\text{LUMO,cal}}^d$ [eV])	$E_{\text{g,CV}}^e$ [eV] ( $E_{\text{g,cal}}^f$ [eV])
<b>3ba</b>	444 (1.0)	0.82	−1.69	−5.62 (−5.31)	−3.11 (−2.36)	2.51 (2.95)
<b>3bb</b>	478 (1.7)	0.80	−1.72	−5.60 (−5.31)	−3.08 (−2.30)	2.52 (3.01)
<b>3db</b>	500 (1.9)	0.71	−1.78	−5.51 (−5.16)	−3.02 (−2.26)	2.48 (2.90)
<b>3ea</b>	613 (0.24)	0.05	−1.82	−4.85 (−4.65)	−2.98 (−2.12)	1.87 (2.52)
<b>3bd</b>	455 (1.5)	1.08	−1.33	−5.88 (−5.79)	−3.47 (−2.92)	2.41 (2.87)
<b>3ed</b>	676 (0.28)	0.16	−1.42	−4.96 (−5.00)	−3.38 (−2.68)	1.58 (2.32)
<b>3fa</b>	600 (0.045)	0.48	−1.60	−5.28 (−5.00)	−3.20 (−2.45)	2.08 (2.55)
<b>3bf</b>	434 (0.68)	0.91	−1.59	−5.71 (−5.50)	−3.21 (−2.51)	2.50 (2.99)
<b>3ff</b>	595 (0.053)	0.61	−1.50	−5.41 (−5.18)	−3.30 (−2.61)	2.11 (2.58)

<sup>a</sup> Measured in  $\text{CH}_2\text{Cl}_2$  ( $1.0 \times 10^{-4} \text{ M}$ ). <sup>b</sup> CV measured with  $\text{Bu}_4\text{NPF}_6$  in  $\text{CH}_2\text{Cl}_2$  ( $1.0 \times 10^{-3} \text{ M}$ ) with a scan rate of  $100 \text{ mV s}^{-1}$  under argon containing  $\text{Ag}/\text{Ag}^+$  as the reference electrode, Pt as the working electrode, and Pt wire as the counter electrode. Values are against  $\text{Fc}/\text{Fc}^+$ . <sup>c</sup>  $E_{\text{HOMO(LUMO),CV}} = -(E_{\text{ox}}^{\text{onset}} + 4.8)$ . <sup>d</sup> Values calculated at the B3LYP/6-31G(d) level of theory. <sup>e</sup>  $E_{\text{g,CV}} = E_{\text{LUMO,CV}} - E_{\text{HOMO,CV}}$ . <sup>f</sup>  $E_{\text{g,cal}} = E_{\text{LUMO,cal}} - E_{\text{HOMO,cal}}$ .

$\epsilon_{\max} = 0.24 \times 10^4 \text{ L mol}^{-1} \text{ cm}^{-1}$ ). TD-DFT calculations suggested that the broad absorption at 613 nm corresponds to the  $\text{HOMO} \Rightarrow \text{LUMO}$  transition ( $f = 0.0355$ ). Furthermore, donor-acceptor type pentalene **3ed** bearing both dimethylamino and nitro groups exhibited a further red shift of  $\lambda_{\max}$  to 676 nm ( $\epsilon_{\max} = 0.28 \times 10^4 \text{ L mol}^{-1} \text{ cm}^{-1}$ ).

A similar phenomenon was observed for the heteroarene-fused pentalenes (Fig. 1c). The absorption spectrum of benzopyridopentalene **3bf** resembled that of dibenzopentalene **3ba**, while benzothienopentalene **3fa** and pyridothienopentalene **3ff** showed new broad absorption bands at around 600 nm, albeit with small  $\epsilon_{\max}$  values (**3fa**:  $\epsilon_{\max} = 4.5 \times 10^2 \text{ L mol}^{-1} \text{ cm}^{-1}$  and **3ff**:  $\epsilon_{\max} = 5.3 \times 10^2 \text{ L mol}^{-1} \text{ cm}^{-1}$ ; Fig. 1c, inset). TD-DFT calculations indicated the positive oscillator strengths corresponding to the  $\text{HOMO} \Rightarrow \text{LUMO}$  transitions for these compounds (**3fa**:  $f = 0.0066$  and **3ff**:  $f = 0.0061$ ), while the oscillator strengths of **3ba** and **3bf** were calculated to be zero ( $f = 0.0000$ ).

Cyclic voltammetry measurement of the obtained pentalenes (**3**) was performed to estimate the energy levels of the highest occupied molecular orbitals (HOMOs) and lowest unoccupied molecular orbitals (LUMOs) (Fig. 2 and Table 2). Symmetric pentalenes, such as dibenzopentalene **3ba** and dinaphthopentalene **3db**, exhibited one reversible oxidation process and one reversible reduction process, whereas an unsymmetric pentalene, benzonaphthopentalene **3bb**,

showed one irreversible oxidation and one reversible reduction (Fig. 2a). Compared with the parent dibenzopentalene **3ba**, dibenzopentalene **3ea** bearing a dimethylamino group exhibited a lower oxidation potential (Fig. 2b), indicating that the introduction of an electron-donating dimethylamino group increased the HOMO level ( $E_{\text{HOMO,CV}} = -4.85 \text{ eV}$  for **3ea** vs.  $-5.62 \text{ eV}$  for **3ba**). On the other hand, the nitro group decreased the LUMO level ( $E_{\text{LUMO,CV}} = -3.47 \text{ eV}$  for **3bd** vs.  $-3.11 \text{ eV}$  for **3ba**) judging from the higher reduction potential of **3bd**. The donor-acceptor type pentalene **3ed** exhibited one reversible oxidation process similar to that of **3ea** and two reversible reduction processes similar to those of **3bd** ( $E_{\text{HOMO,CV}} = -4.96 \text{ eV}$  and  $E_{\text{LUMO,CV}} = -3.38 \text{ eV}$ ). This corresponds to a HOMO-LUMO gap of 1.58 eV, which is the narrowest among donor-acceptor-type dibenzo[*a,e*]pentalene derivatives ever reported.<sup>5b,12</sup> With regard to the heteroarene-fused derivatives, benzothienopentalene **3fa** exhibited relatively high HOMO and low LUMO energy levels ( $E_{\text{HOMO,CV}} = -5.28 \text{ eV}$  and  $E_{\text{LUMO,CV}} = -3.20 \text{ eV}$ ; Fig. 2c), indicating that the replacement of one of the fused benzene rings of dibenzo[*a,e*]pentalene by a thiophene ring results in a narrower HOMO-LUMO energy gap. The introduction of a pyridine ring, on the other hand, shows a different electronic effect. Thus, compared with **3ba** and **3fa**, benzopyridopentalene **3bf** and pyridothienopentalene **3ff** showed lower LUMO and HOMO energy levels with similar energy gaps, respectively.

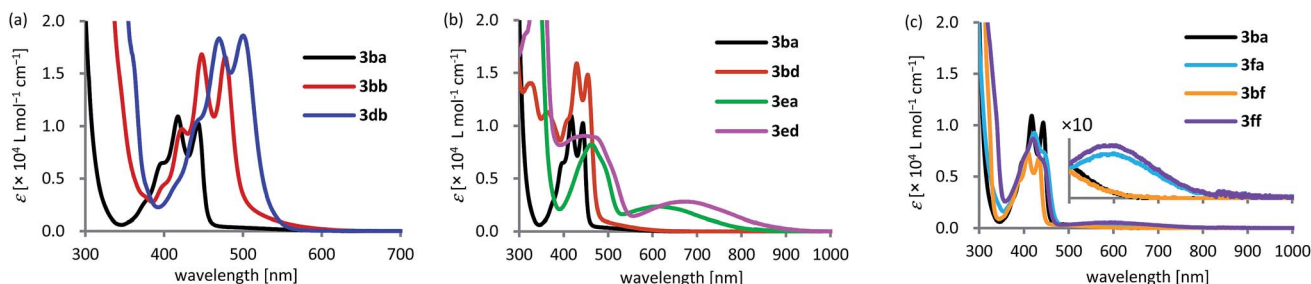


Fig. 1 UV-vis absorption spectra of (a) **3ba**, **3bb**, and **3db**, (b) **3ba**, **3bd**, **3ea**, and **3ed**, and (c) **3ba**, **3fa**, **3bf**, and **3ff** in  $\text{CH}_2\text{Cl}_2$  ( $1.0 \times 10^{-4} \text{ M}$ ) at  $25^\circ \text{C}$ .



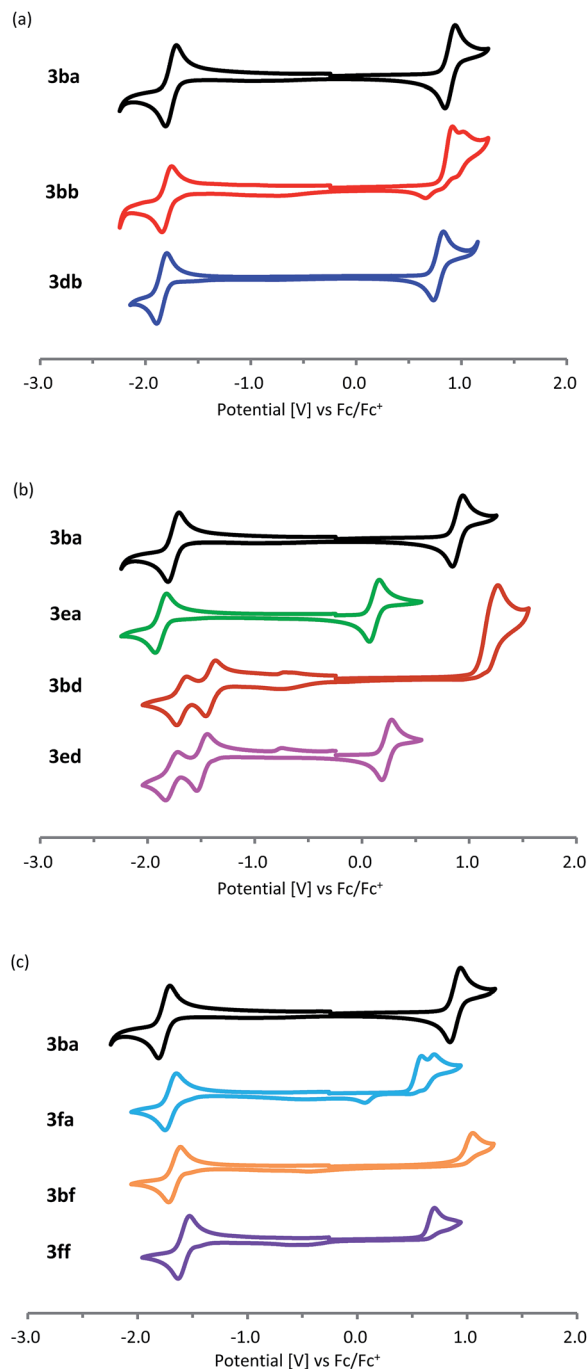


Fig. 2 Cyclic voltammograms of (a) **3ba**, **3db**, and **3bb**, (b) **3ba**, **3ea**, **3bd**, and **3ed**, and (c) **3ba**, **3fa**, **3bf**, and **3ff** measured with  $\text{Bu}_4\text{NPF}_6$  in  $\text{CH}_2\text{Cl}_2$  (0.1 M) with a scan rate of  $100 \text{ mV s}^{-1}$  under argon containing  $\text{Ag}/\text{Ag}^+$  as the reference electrode, Pt as the working electrode, and Pt wire as the counter electrode. The potential was externally calibrated against  $\text{Fc}/\text{Fc}^+$ .

The origin of the electronic effects caused by the introduction of thiophene and pyridine rings was assessed by comparing the calculated nucleus-independent chemical shift (NICS) values of compounds **3ba**, **3fa**, and **3ff** (B3LYP/6-31G(d); Fig. 3). The NICS(0) values of the central five-membered rings indicate that the antiaromaticity of thiophene-fused **3fa** and **3ff** is higher

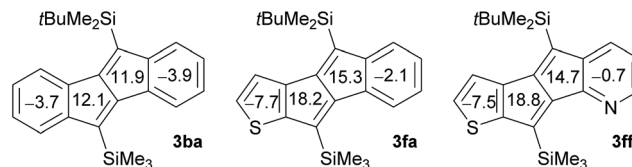


Fig. 3 NICS(0) values of **3ba**, **3fa**, and **3ff** (B3LYP/6-31G(d)).

than that of dibenzopentalene **3ba**, which leads to the narrower HOMO–LUMO gaps. Pentalenes that are fused by heteroles, such as thiophene and pyrrole, *via* the b bond are known to have higher antiaromaticity, because the contribution of the resonance structure with isolated  $8\pi$ -electrons becomes more dominant.<sup>4d,9b,10b</sup> On the other hand, the negligible effect of the pyridine ring on the NICS(0) values can explain the similar HOMO–LUMO gaps of **3fa** and **3ff**.

## Conclusions

In summary, we have developed a novel method for the synthesis of dibenzo[*a,e*]pentalene derivatives using a rhodium-catalysed stitching reaction. The introduction of appropriately sized silyl groups on the starting substrates led to a high crossover selectivity without using an excess amount of either substrate. Various unsymmetric dibenzo[*a,e*]pentalene derivatives, including those with electronically different substituents on the fused benzene rings as well as heteroarene fused compounds, could be synthesised using the present catalysis. The obtained pentalenes can also be transformed into halogenated pentalenes by desilylative halogenation reactions. The optical and electronic properties of these dibenzo[*a,e*]pentalene derivatives were also examined, and the novel donor–acceptor type pentalene **3ed** bearing dimethylamino and nitro groups exhibited a small HOMO–LUMO gap of 1.58 eV.

## Acknowledgements

This work was supported in part by a Grant-in-Aid for Young Scientists (A) (S.I.: No. 16H06030), a Grant-in-Aid for Challenging Exploratory Research (R.S.: 15K13688), and “Nanotechnology Platform” (project No. 12024046), MEXT, Japan, and in part by JGC-S Scholarship Foundation (R.S.) and Asahi Glass Foundation (R.S.). K. T. would like to thank the Japan Society for the Promotion of Science (JSPS) for their Program for Leading Graduate Schools (MERIT), and for a Research Fellowship for Young Scientists. The theoretical calculations were performed using computational resources provided by Research Center for Computational Science, National Institutes of Natural Sciences, Okazaki, Japan.

## Notes and references

- (a) H. Hopf, *Angew. Chem., Int. Ed.*, 2013, **52**, 12224; (b) H. Hopf, *Classics in Hydrocarbon Chemistry*, Wiley-VCH, Weinheim, 2000, p. 277.



- 2 (a) K. Hafner, R. Dönges, E. Goedecke and R. Kaiser, *Angew. Chem., Int. Ed. Engl.*, 1973, **12**, 337; (b) R. Dönges, K. Hafner and H. J. Lindner, *Tetrahedron Lett.*, 1976, **17**, 1345.
- 3 For reviews: (a) T. Kawase and J.-i. Nishida, *Chem. Rec.*, 2015, **15**, 1045; (b) M. Saito, *Symmetry*, 2010, **2**, 950; (c) M. Rabinovitz, I. Willner and A. Minsky, *Acc. Chem. Res.*, 1983, **16**, 298.
- 4 (a) T. Kawase, T. Fujiwara, C. Kitamura, A. Konishi, Y. Hirao, K. Matsumoto, H. Kurata, T. Kubo, S. Shinamura, H. Mori, E. Miyazaki and K. Takimiya, *Angew. Chem., Int. Ed.*, 2010, **49**, 7728; (b) G. Dai, J. Chang, W. Zhang, S. Bai, K.-W. Huang, J. Xu and C. Chi, *Chem. Commun.*, 2015, **51**, 503; (c) C. Li, C. Liu, Y. Li, X. Zhu and Z. Wang, *Chem. Commun.*, 2015, **51**, 693; (d) G. Dai, J. Chang, X. Shi, W. Zhang, B. Zheng, K.-W. Huang and C. Chi, *Chem.-Eur. J.*, 2015, **21**, 2019.
- 5 (a) G. Babu, A. Orita and J. Otera, *Chem. Lett.*, 2008, **37**, 1296; (b) F. Xu, L. Peng, A. Orita and J. Otera, *Org. Lett.*, 2012, **14**, 3970. See also: (c) M. Chakraborty, C. A. Tessier and W. J. Youngs, *J. Org. Chem.*, 1999, **64**, 2947; (d) F. Xu, L. Peng, K. Wakamatsu, A. Orita and J. Otera, *Chem. Lett.*, 2014, **43**, 1548; (e) S. Nobusue, A. Yoshizaki, M. Miki, H. Miyoshi, A. Shimizu and Y. Tobe, *Tetrahedron*, 2014, **70**, 8474; (f) F. Xu, L. Peng, K. Shinohara, T. Nishida, K. Wakamatsu, M. Uejima, T. Sato, K. Tanaka, N. Machida, H. Akashi, A. Orita and J. Otera, *Org. Lett.*, 2015, **17**, 3014.
- 6 (a) M. Saito, M. Nakamura, T. Tajima and M. Yoshioka, *Angew. Chem., Int. Ed.*, 2007, **46**, 1504; (b) H. Li, B. Wei, L. Xu, W.-X. Zhang and Z. Xi, *Angew. Chem., Int. Ed.*, 2013, **52**, 10822; (c) H. Li, X.-Y. Wang, B. Wei, L. Xu, W.-X. Zhang, J. Pei and Z. Xi, *Nat. Commun.*, 2014, **5**, 4508.
- 7 H. Zhang, T. Karasawa, H. Yamada, A. Wakamiya and S. Yamaguchi, *Org. Lett.*, 2009, **11**, 3076.
- 8 (a) C. Chen, M. Harhausen, R. Liedtke, K. Bussmann, A. Fukazawa, S. Yamaguchi, J. L. Petersen, C. G. Daniliuc, R. Fröhlich, G. Kehr and G. Erker, *Angew. Chem., Int. Ed.*, 2013, **52**, 5992; (b) C. Chen, M. Harhausen, A. Fukazawa, S. Yamaguchi, R. Fröhlich, C. G. Daniliuc, J. L. Petersen, G. Kehr and G. Erker, *Chem.-Asian J.*, 2014, **9**, 1671.
- 9 (a) T. Kawase, A. Konishi, Y. Hirao, K. Matsumoto, H. Kurata and T. Kubo, *Chem.-Eur. J.*, 2009, **15**, 2653; (b) A. Konishi, T. Fujiwara, N. Ogawa, Y. Hirao, K. Matsumoto, H. Kurata, T. Kubo, C. Kitamura and T. Kawase, *Chem. Lett.*, 2010, **39**, 300.
- 10 (a) Z. U. Levi and T. D. Tilley, *J. Am. Chem. Soc.*, 2009, **131**, 2796; (b) X. Yin, Y. Li, Y. Zhu, Y. Kan, Y. Li and D. Zhu, *Org. Lett.*, 2011, **13**, 1520.
- 11 T. Maekawa, Y. Segawa and K. Itami, *Chem. Sci.*, 2013, **4**, 2369.
- 12 J. Zhao, K. Oniwa, N. Asao, Y. Yamamoto and T. Jin, *J. Am. Chem. Soc.*, 2013, **135**, 10222.
- 13 R. Shintani, R. Iino and K. Nozaki, *J. Am. Chem. Soc.*, 2016, **138**, 3635.
- 14 For review articles on related rhodium-catalyzed carbon-carbon bond-forming reactions, see: (a) M. M. Heravi, M. Dehghani and V. Zadsirjan, *Tetrahedron: Asymmetry*, 2016, **27**, 513; (b) M. Shiotsuki, F. Sanda and T. Masuda, *Polym. Chem.*, 2011, **2**, 1044; (c) H. J. Edwards, J. D. Hargrave, S. D. Penrose and C. G. Frost, *Chem. Soc. Rev.*, 2010, **39**, 2093; (d) T. Aoki, T. Kaneko and M. Teraguchi, *Polymer*, 2006, **47**, 4867; (e) M. G. Mayershofer and O. Nuyken, *J. Polym. Sci., Part A: Polym. Chem.*, 2005, **43**, 5723; (f) *Modern Rhodium-Catalyzed Organic Reactions*, ed. P. Andrew Evans, Wiley-VCH, Weinheim, 2005; (g) T. Hayashi and K. Yamasaki, *Chem. Rev.*, 2003, **103**, 2829; (h) K. Fagnou and M. Lautens, *Chem. Rev.*, 2003, **103**, 169.
- 15 The use of the corresponding arylboronic acid or its pinacol ester instead of the neopentyl glycol ester produced dibenzo [a,e]pentalenes in comparable yields. See ESI† for details.
- 16 (a) T. Hayashi, K. Inoue, N. Taniguchi and M. Ogasawara, *J. Am. Chem. Soc.*, 2001, **123**, 9918; (b) M. Lautens and M. Yoshida, *Org. Lett.*, 2002, **4**, 123; (c) T. Fujii, T. Koike, A. Mori and K. Osakada, *Synlett*, 2002, 295; (d) Y. Nakao, M. Takeda, J. Chen and T. Hiyama, *Synlett*, 2008, 774.
- 17 (a) T. Miura, M. Yamauchi and M. Murakami, *Synlett*, 2007, 2029; (b) L. Artok, M. Kuş, B. N. Ürer, G. Türkmen and Ö. Aksn-Artok, *Org. Biomol. Chem.*, 2010, **8**, 2060.
- 18 (a) K. Ueura, T. Satoh and M. Miura, *Org. Lett.*, 2005, **7**, 2229; (b) R. Shintani, T. Yamagami and T. Hayashi, *Org. Lett.*, 2006, **8**, 4799; (c) S. D. Timpa, C. M. Fafard, D. E. Herbert and O. V. Ozerov, *Dalton Trans.*, 2011, **40**, 5426; (d) Y. J. Jang, H. Yoon and M. Lautens, *Org. Lett.*, 2015, **17**, 3895.
- 19 F. Xu, L. Peng, K. Wakamatsu, A. Orita and J. Otera, *Chem. Lett.*, 2014, **43**, 1548.
- 20 S. Nagakura and J. Tanaka, *J. Chem. Phys.*, 1954, **22**, 236.

